

Comparative Analysis of Solder Joint Degradation Using RF Impedance and Event Detectors

Daeil Kwon¹, Michael H. Azarian¹, and Michael Pecht^{1,2}

¹Center for Advanced Life Cycle Engineering (CALCE)

University of Maryland

College Park, MD 20742, USA

Phone: +1-301-405-5323, FAX: +1-301-314-9269

²Prognostics and Health Management Center

City University of Hong Kong

Kowloon, Hong Kong

Abstract

Under cycling loading conditions, solder joints are susceptible to fatigue cracking, which often initiates at the surface where the strain range is maximized. Event detectors have been widely used to detect failure of solder joints during reliability testing. These devices monitor DC resistance using very high sampling rates, thus allowing failure to be defined on the basis of a minimum number of samples that exceed a failure threshold. Event detectors excel at recording rapid, intermittent changes in resistance and identifying a DC open circuit, which is the typical criterion for failure. However, event detectors are not sensitive to early stages of degradation, because changes in resistance under cyclic loading conditions do not occur until a crack has propagated almost all the way through a solder joint, and because their sensitivity to small changes in DC resistance is adversely affected by temperature variations and electromagnetic interference.

RF impedance monitoring offers a highly sensitive means of detecting interconnect degradation. Due to the skin effect, a phenomenon wherein signal propagation at high frequencies is concentrated near the surface of a conductor, even a small crack initiating at the surface of a solder joint raises the RF impedance. Thus, RF impedance monitoring can detect early stages of solder joint degradation long before it results in a DC open circuit.

In order to compare the respective sensitivities in detecting solder joint degradation between RF impedance and event detectors, mechanical fatigue tests have been conducted with an impedance-controlled circuit board on which a surface mount component was soldered. During cyclic loading, simultaneous measurements were taken of DC resistance and the reflection coefficients obtained from time domain reflectometry (TDR) as a measure of RF impedance. The TDR reflection coefficients were consistently observed to increase in response to early stages of solder joint cracking prior to the first failure detection of an event detector. The results demonstrate that RF impedance monitoring has the potential to predict and prevent failures of electronic products due to solder joint cracking by providing a warning that an interconnect has begun to degrade.

Introduction

The reliability of an electronic package is largely affected by the durability of interconnects such as solder joints. One of the most common failure modes is a DC open circuit due to solder joint cracking, which generally initiates from the circumferential area where the strain energy is maximized and propagates inward [1][2]. A cracked solder joint sometimes is extremely hard to detect when it is part of a daisy-chain and is surrounded by other solder joints that have not cracked yet. This cracked solder joint may seem to provide a good electrical contact due to the compressive load applied by the neighboring intact joints, but it can cause the occasional loss of electrical continuity under operational and environmental loading conditions [3]. Thus, cracked solder joints can lead to an intermittent failure of the package and eventually a permanent failure of the product or system.

The electronics industry has long been using event detectors and data loggers to detect intermittent behavior of solder joint resistance under loading conditions [3][4]. In general, changes in DC resistance in response to solder joint degradation can be detected by these instruments only after a crack has propagated almost all the way across the solder joint [5]. However, it has been previously reported that RF impedance exhibits increased sensitivity in detecting early stages of solder joint degradation compared to DC resistance [6][7]. While a small crack at the surface of a solder joint would not affect DC resistance, it can raise the RF impedance due to the skin effect, a phenomenon wherein signal propagation at high frequencies is concentrated near the surface of a conductor.

This paper compares the respective sensitivities in detecting early stages of solder joint degradation of RF impedance and event detectors. A test circuit was designed to simultaneously monitor both RF impedance and event detector measurements. Mechanical fatigue tests were performed on an impedance-controlled circuit board containing a surface mount component. In the following sections, detailed experimental procedures are discussed, and a comparative analysis between RF impedance and event detector measurements is presented.

Early detection of solder joint degradation

Paired with measurements taken using event detectors or data loggers, the IPC-SM-785 standard is widely used in the electronics industry to define the criteria for solder joint failure during reliability or qualification testing of electronics [8]. An event is defined to be a loss of electrical continuity where the resistance of the circuit exceeds a threshold resistance (R_{th}), which is also defined by the standard. The standard defines a failure as the first event (t_0) associated with the loss of electrical continuity, if it is followed by nine additional events within an additional 10% of the lifetime ($t_0+0.1t_0$) as shown in Figure 1. The loss of electrical continuity of a solder joint typically occurs when a crack within the solder joint is large enough to result in an instantaneous open circuit due to operational or environmental loading conditions. Because of their rapid sampling rate, event detectors are also widely believed to be the best means of detecting a crack under cyclic or transient loading conditions. Nevertheless, event detectors may not be useful for detecting early stages of solder joint degradation, since the resistance increase associated with a partial crack would not be large enough to trigger an event.

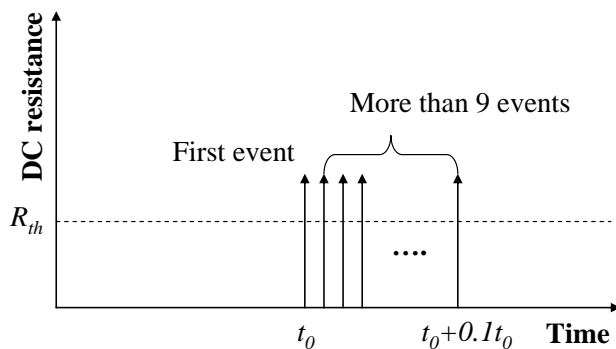


Figure 1: Schematic representation of failure definition according to IPC-SM-785

RF impedance can be used as an alternative means of detection that exhibits increased sensitivity to changes at the surface of a solder joint. At frequencies of several hundred MHz or more, signal propagation is more sensitive to changes at the surface of a conductor, such as a solder joint, due to surface concentration of the current, which is known as the skin effect. “Skin depth” refers to the thickness of the conductor within which about 63% of the current is contained [9]. As shown in equation (1), the skin depth, δ , is directly related to the frequency, f , and the resistivity of the conductor, ρ :

$$\delta = \sqrt{\frac{\rho}{f \pi \mu}} \quad (1)$$

where μ denotes the material’s permeability. Due to the skin effect, the current density falls off exponentially with distance from the surface of a conductor. More than 99% of the current is concentrated within 5 skin depths of the surface. Figure 2 shows the cumulative current density over distance from the surface of a conductor. This surface concentration of current makes RF impedance more sensitive to mechanical degradation, such as a crack, at the periphery of a solder joint.

In this study, time domain reflectometry (TDR) was used as a measure of RF impedance. TDR is useful for identifying fault locations in a circuit because it provides information about the magnitude and sign of impedance variations as well as localizing their positions within the circuit. A TDR measurement is conducted by injecting a pulse or waveform into a circuit and monitoring the reflected voltages due to impedance discontinuities within the circuit as well as the round-trip transit time to the location of these discontinuities. A reflection coefficient (Γ) is often used to report the magnitude of a TDR measurement. The reflection coefficient is the ratio of the reflected voltage to the signal voltage transmitted from the same port, and it is expressed as shown in equation (2):

$$\Gamma = \frac{V_{reflected}}{V_{incident}} = \frac{Z_L - Z_0}{Z_L + Z_0} \quad (2)$$

where Z_L and Z_0 denote the impedance of the device under test (DUT) and the characteristic impedance of the circuit, respectively.

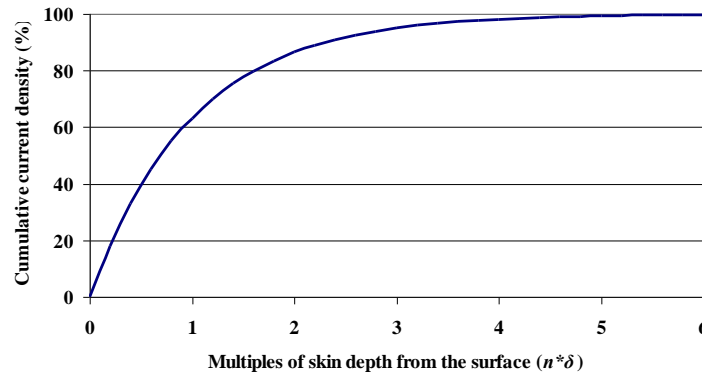


Figure 2: Cumulative current density vs. multiples of skin depth from the surface

In order to compare the respective sensitivities in detecting solder joint degradation, simultaneous measurements were performed of the TDR reflection coefficients and an event detector, while the solder joints in a test circuit were stressed by a cyclic mechanical shear force.

Experimental setup and test conditions

A test circuit was developed to simultaneously monitor both the TDR reflection coefficient and the event detector measurement during solder joint degradation. As shown in Figure 3, the test circuit consisted of an impedance-controlled circuit board, two bias-tees, RF cables, a uniaxial load tester, and measurement instruments. The circuit board has a controlled characteristic impedance of 50 Ohms to match that of the measurement instruments and other components. A surface mount technology (SMT) low pass filter was soldered onto this circuit board using eutectic tin-lead (Sn-37Pb) solder. The low pass filter has a cut-off frequency of 6.7 GHz. Since the monitored frequency range for the TDR reflection coefficient measurement was between 500 MHz and 6 GHz, the filter acted as a conductor with the same characteristic impedance of 50 Ohms.

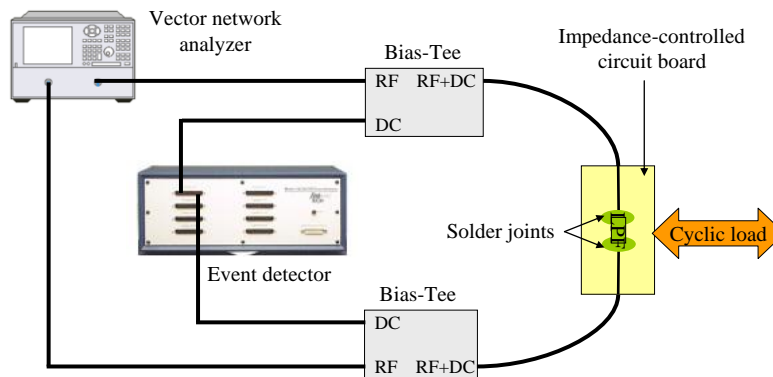


Figure 3: Schematic of test circuit for simultaneous monitoring of TDR reflection coefficient and event detector measurement

An MTS Tytron 250 was used to generate a cyclic shear force to produce fatigue failures of the solder joint. Based on the shear strength measurement of the solder joint and several preliminary test results, a sinusoidal load profile was selected, with an amplitude of 10 N and a frequency of 0.25 Hz, superimposed on an offset force of 30 N, as shown in Figure 4. The offset force maintained the contact between the component and the load transducer. A load probe was attached to the end of the transducer and made contact with the component through a strip of alumina, which was inserted in order to avoid introducing electrical interference at the point of contact. Figure 5 shows the test apparatus focusing on the test vehicle and the load transducer.

An AnalysisTech STD128 event detector was used to continuously monitor the DC continuity of the test circuit. A threshold resistance of 1000 Ohms was configured according to the IPC-SM-785 standard [7]. The effects of the high frequency signals and the RF components on the event detector measurement were evaluated to determine whether the event detector

might be affected by signals of a few gigahertz or the bias-tees. By intentionally introducing an electrical discontinuity into the test circuit, it was confirmed that the operation of the event detector was not influenced by the high frequency signals and components used in this study.

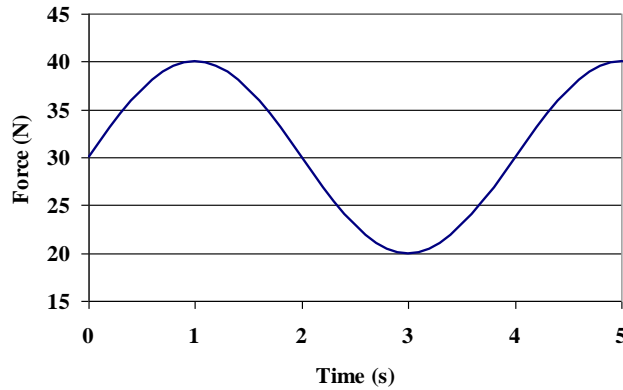


Figure 4: Cyclic shear force profile

An Agilent E8364A vector network analyzer (VNA) was used to monitor the TDR reflection coefficient during solder joint degradation. For TDR reflection coefficient measurement, the VNA swept and collected the reflection coefficients across the defined frequency range and then applied an inverse fast Fourier transform. Therefore, the time domain measurement using a network analyzer is a composite response over all the frequencies monitored.

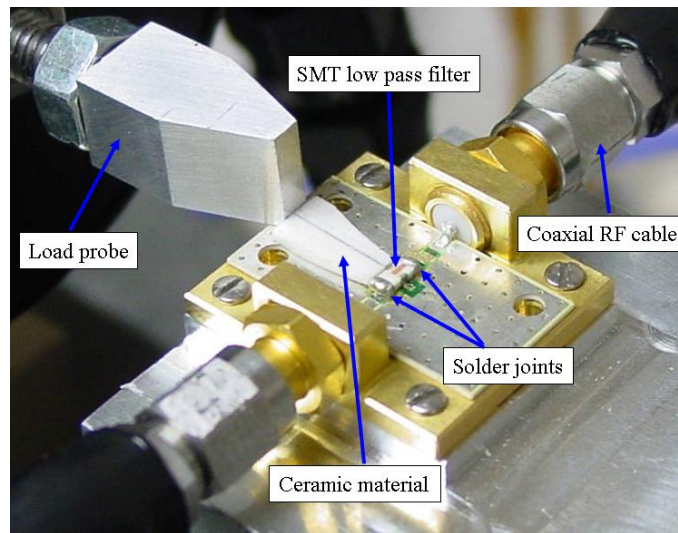


Figure 5: Test apparatus

Test results

Fatigue tests were conducted by applying a cyclic shear force to the component with simultaneous monitoring of the TDR reflection coefficient and the alarm status of the event detector. Each experiment was performed until the applied force resulted in a DC open circuit. The event detector polled out a measurement result once per second, and it triggered an alarm when the monitored DC resistance exceeded the threshold resistance. Thus, the output value from the event detector was either zero or one, indicating either a short or an open circuit, respectively. The TDR reflection coefficient was collected every 30 seconds using instrumental control software. Each set of TDR measurements contained a collection of reflection coefficient values over the signal path of the circuit board. In order to compare them with the event detector measurements, the TDR reflection coefficients at the solder joint were extracted and displayed in one plot as a function of test duration.

Figure 6 shows test results in which the solder joint failed by fatigue due to the application of the cyclic shear force. The duration of the test was 4307 minutes, at which time a DC open circuit of the solder joint was observed. Around the beginning of the test, the TDR reflection coefficient remained at its initial value. However, toward the end of the test, it gradually increased and eventually exhibited an abrupt increase, which indicated a DC open circuit. Within the curve that the

TDR reflection coefficient produced, a 5% increase of the initial value occurred at 4260 minutes, which was 47 minutes earlier than the time to failure based on the event detector. The event detector did not trigger any alarms in response to intermittent behavior of DC resistance prior to the DC open circuit.

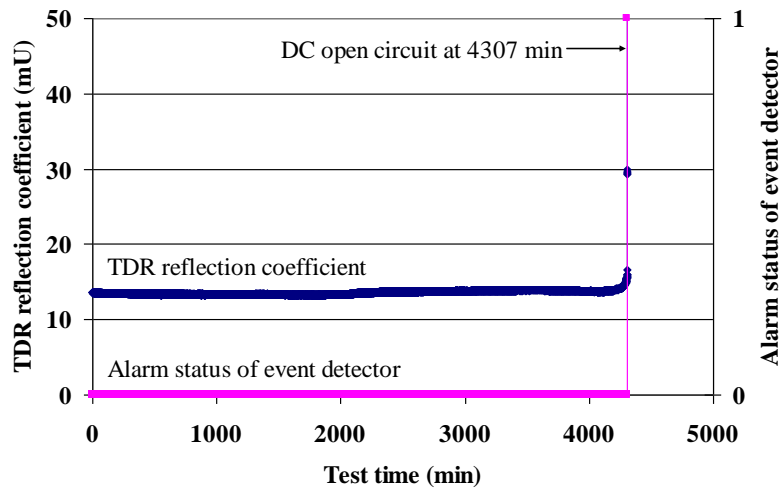


Figure 6: Comparison between the TDR reflection coefficient and the alarm status of the event detector during a fatigue test

Figure 7 is a photograph of the cracked solder joint taken after the fatigue test. The direction of the solder joint separation coincided with that of the applied shear force. The failure mode was confirmed to be a DC open circuit at the solder joint by measuring a DC resistance after the failure, and the failure mechanism was the solder joint cracking that propagated all the way across the solder joint. In general, the same behaviors of the TDR reflection coefficient and the event detector measurement were consistently observed over multiple trials, along with the confirmation of the same failure mechanism, solder joint cracking.



Figure 7: Cracked solder joint due to the application of the cyclic shear force after the fatigue test

Conclusions

This study demonstrated that RF impedance is more sensitive to mechanical degradation of a solder joint than an event detector. A test vehicle was developed to allow direct comparison of the respective sensitivities between TDR reflection coefficients as a measure of RF impedance and an event detector during the generation of mechanical fatigue failure of the solder joints on the test vehicle. The test results showed that the TDR reflection coefficients were consistently observed to increase in response to early stages of solder joint degradation prior to the first failure detection of the event detector. This indicates that the TDR reflection coefficient can serve as a dependable solder joint failure indicator in spite of its low speed sampling compared to the event detector, which performs continuous high speed sampling.

These test results imply that reliability assessment based on DC resistance measurements, using equipment such as event detectors, may overestimate the lifetime of high speed electronic assemblies. As the characteristic frequencies of transmitted signals increase beyond several hundred MHz or more, the performance of electronic assemblies will be increasingly sensitive to even minor levels of interconnect damage, such as solder joint cracking. As shown in the test results, RF impedance can provide a more sensitive means to diagnose solder joint degradation than do measurements based on DC

resistance. Thus, measuring RF impedance allows for more accurate assessment of the reliability of high speed electronic products.

Another implication of these findings is that RF impedance can serve as a prognostic tool, providing the remaining useful life of electronic products. Since the changes in TDR reflection coefficient leading up to failure were gradual in nature, it should be possible to quantify the damage level associated with solder joint cracking. An appropriate threshold that exceeds an acceptable solder joint damage level can trigger an alarm to provide condition-based maintenance, thereby increasing product safety and availability along with substantial savings in the lifecycle cost of a product.

Future work on this topic will involve quantification of the relationship between physical degradation and RF impedance, and testing of more complex test vehicles and interconnect structures under a variety of environmental and operational loading conditions.

Acknowledgement

This work was funded by the members of the CALCE Electronic Products and Systems Consortium at the University of Maryland.

References

- [1] Pecht, M., McCluskey, P., and Evans, J., "Failures in Electronic Assemblies and Devices," in *Product Integrity and Reliability in Design*, J. Evans, and J. Evans, Eds., London: Springer-Verlag, 2001, pp. 204-232.
- [2] Andersson, C., Andersson, D., Tegehall, P., and Liu, J., "Effect of Different Temperature Cycle Profiles on the Crack Propagation and Microstructural Evolution of Lead Free Solder Joints of Different Electronic Components," *Thermal and Mechanical Simulation and Experiments in Micro-electronics and Micro-systems*, Brussels, Belgium, May 2004.
- [3] Qi, H., Vichare, N., Azarian, M. H., and Pecht, M., "Analysis of Solder Joint Failure Criteria and Measurement Techniques in the Qualification of Electronic Products," *IEEE Trans. on Components and Packaging Technologies*, vol. 31, no. 2, 2008, pp. 469-477.
- [4] Guédon-Gracia, A., Woïrgard, E., and Zardini, C., "Reliability of Lead-Free BGA Assembly: Correlation between Accelerated Ageing Tests and FE Simulations," *IEEE Trans. on Device and Materials Reliability*, vol. 8, no. 3, pp. 449-454, 2008.
- [5] Caers, J. F. J. M., Wong, E. H., Seah, S. K. W., Zhao, X., J., Selvanayagam, C. S., Driel., W. D.van, Owens., N., Leoni, M., Tan, L. C., Eu, P. L., Lai, Y., and Yeh, C., "A Study of Crack Propagation in Pb-free Solder Joints under Drop Impact," *IEEE Electronic Components and Technology Conference*, Orlando, FL, May 2008.
- [6] Kwon, D., Azarian, M. H., and Pecht, M., "Early Detection of Interconnect Degradation by Continuous Monitoring of RF Impedance," *IEEE Trans. on Device and Materials Reliability*, vol. 9, no. 2, pp. 296-304, 2009.
- [7] Azarian, M. H, Kwon, D., and Pecht, M., "Use of the Skin Effect for Detection of Interconnect Degradation," *International Symposium on Microelectronics and Electronics Packaging*, San Jose, CA, Nov. 2009.
- [8] Guidelines for Accelerated Reliability Testing of Surface Mount Solder Attachments, IPC-SM-785 Standard, 1992.
- [9] Thierauf, S. C., *High-Speed Circuit Board Signal Integrity*, Massachusetts: Artech House Inc., 2004.

Table 2. Results of regression on the capacitance data (for group A capacitors) at 125°C and 285 V

Aging condition	Linear degradation region			Logarithmic degradation region		
	m	C_o	r^2	k	C_{o1}	r^2
125°C, 285 V	-5.09E-14	4.34E-10	0.48	-7.20E-11	7.84E-10	0.95

Statistical analysis was performed on the time-to-failure data (as a result of a decrease in the capacitance) for small capacitors. A Weibull 3-parameter distribution was fitted to the failure data as shown in Fig. 8, and the parameters of the distribution are given in Table 3, where γ is the location parameter. The value of time to 50 percent failure (t_{50}) at 125°C and 285 V aging was found to be 392.4 hrs.

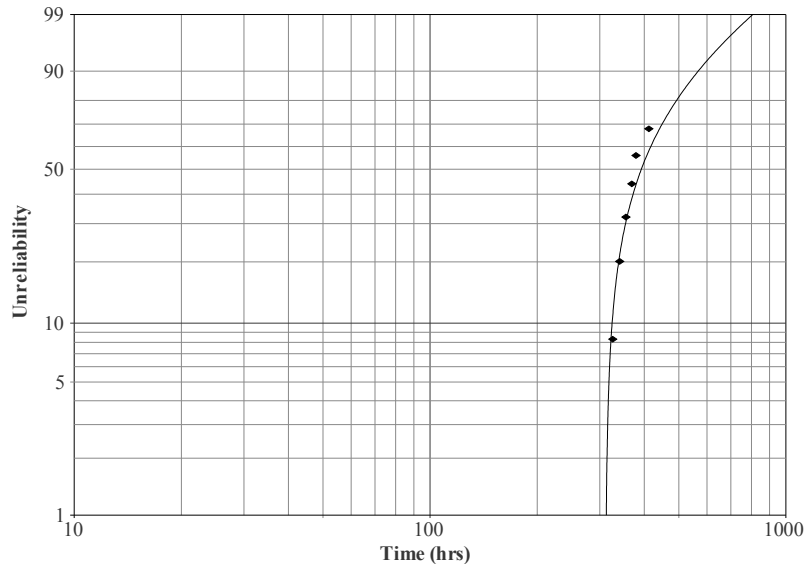


Fig. 8. Unreliability vs. time-to-failure due to capacitance decrease (for group A capacitors) at 125°C and 285 V

Table 3. Statistical analysis of time-to-failure due to capacitance decrease (for group A capacitors)

Aging condition	Test duration (hrs)	Failed	Survived	t_{50} (hrs)	β	η	γ
125°C and 285V	500	6	2	392	1.04	115	312

No failures as a result of decrease in capacitance were observed for large capacitors (group B) at 125°C and 285 V. The degradation in the capacitance for large capacitors was different as compared to small capacitors, and no linear degradation region was found as shown in Fig. 9. The values of constants C_{o1} and k for the logarithmic degradation were found by regression and are presented in Table 4.

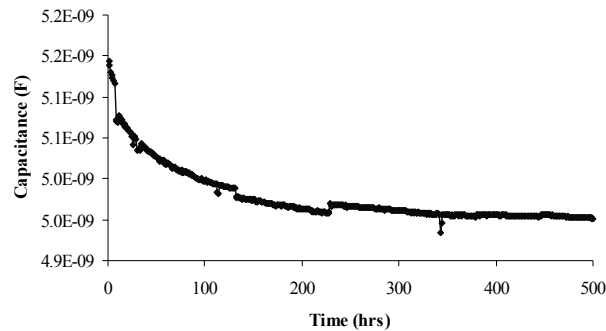


Fig. 9. Typical plot of capacitance (for group B capacitors) at 125°C and 285 V

Table 4. Results of regression on the capacitance data (for group B capacitors) at 125°C and 285 V

Aging condition	Logarithmic degradation region		
	k	C ₀₁	r ²
125°C, 285 V	-4.13E-11	5.10E-9	0.96

The values of the constant k for the logarithmic degradation rate for small and large capacitors are comparable to each other implying that the logarithmic degradation was due to a change in the material properties of the dielectric. The time-to-failure (TTF) as a result of a decrease (20%) in capacitance in the logarithmic degradation region can be computed by:

$$TTF = \ln^{-1}\left(\frac{0.8C_{01}}{k}\right) \quad (5)$$

Since the initial value of capacitance (C_{01}) of large capacitors was around one order of magnitude higher than the capacitance of small capacitors and the value of k was found to be comparable, no failures were observed in large capacitors during the duration of test.

In the future, temperature and voltage tests will be conducted at 125°C, 250V and 105°C, 285V and the values of Prokopowicz constants will be computed. Since failures were also observed as a result of a decrease in capacitance, a model for the TTF (as a result of a decrease in capacitance) will be developed.

6 Temperature-humidity-bias tests

The objective of conducting temperature-humidity-bias tests was to investigate the effects of an applied voltage under elevated temperature and humidity conditions. Three test vehicles were biased at 0, 5, and 150 V in an environmental chamber maintained at 85°C and 85% RH. 36 out of 80 capacitors were selected from group A (small capacitors) and 4 out of 6 capacitors were selected from group B (large capacitors). The parameters of 120 capacitors were monitored in-situ every one hour.

Thus far 395 hours of testing have been completed and the test is still proceeding. No failures were observed in the test vehicle that was biased at 0 and 5 V. At both these stress levels the capacitance was found to increase with time, as expected. Typical plots of the capacitance of group A and group B capacitors (maintained at 85°C and 85% RH) are shown in Fig. 10 and Fig. 11, respectively. It can be observed that for small capacitors (group A) the capacitance stabilized within the first 100 hrs, whereas in large capacitors (group B) the capacitance is still increasing. The reason for this behavior is currently under investigation.

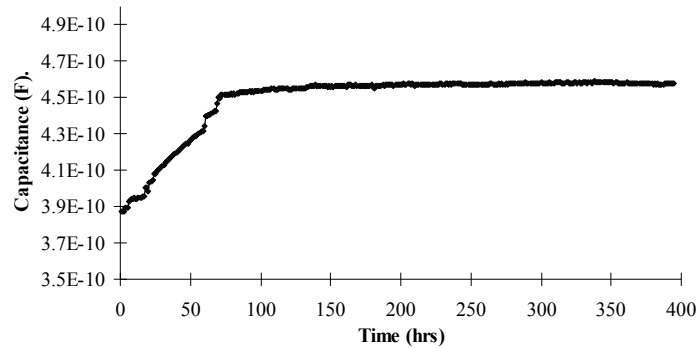


Fig. 10. Capacitance of group A capacitors (maintained at 85°C, 85% RH, and 0 V)

The average increase in capacitance after 395 hrs for group A and group B capacitors maintained at 85°C, 85% RH and 85°C, 85% RH, and 5 V are given in Table 5. The dissipation factor was also found to increase due to moisture absorption in the dielectric.

Table 5. Percentage increase in capacitance

Stress level	Group A	Group B
85°C and 85% RH	17.3 ± 1.7	13.9 ± 0.5
85°C, 85% RH, and 5 V	17.3 ± 1.7	13.8 ± 0.6

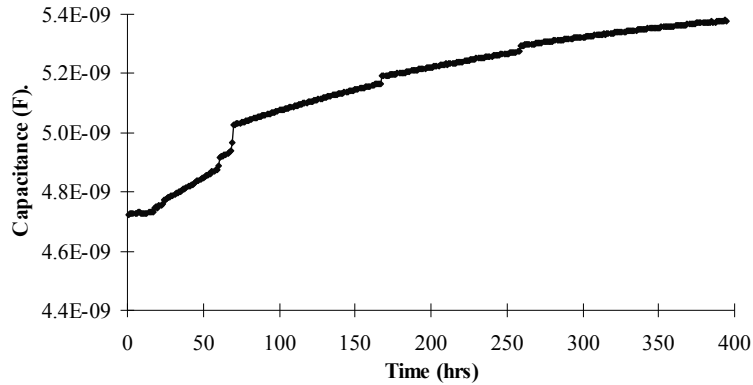


Fig. 11. Capacitance of group B capacitors (maintained at 85°C, 85% RH, and 0 V)

Insulation resistance was found to increase on both test vehicles (that were biased at 0 and 5 V) and is shown in Fig. 12. The reason for this increase in insulation resistance under humid conditions is currently under investigation.

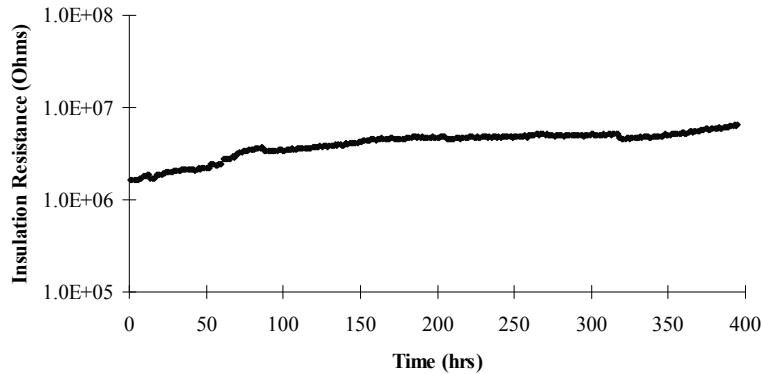


Fig. 12. Insulation resistance of group A capacitors (maintained at 85°C, 85% RH, and 0 V)

Failures were observed due to a sharp drop in insulation resistance on the test vehicle that was biased at 150 V. A typical plot of insulation resistance of a failed capacitor is shown in Fig. 13. Many intermittent failures were observed before the permanent failure. 32 out of 36 capacitors of group A and 4 out of 4 capacitors of group B failed within 395 hrs. The value of capacitance started to fluctuate after failure (as a result of a sharp drop in IR), so the increase in capacitance at this stress level is not calculated. The THB test at 150 V bias will be terminated upon failure of the remaining capacitors of group A.

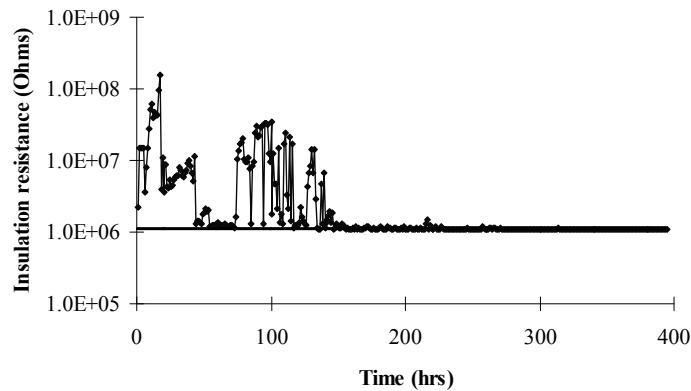


Fig. 13. Insulation resistance of group A capacitors (maintained at 85°C, 85% RH, and 150 V)

The THB test at 0 and 5 V bias will be continued for up to 2500 hrs or complete failure of all capacitors (whichever is earlier). Any differences in the measured parameters of the boards biased at 0 and 5 V will be analyzed.

7 Conclusions

The reliability of an embedded capacitor with epoxy-BaTiO₃ composite dielectric (8 μm thick) was investigated during temperature and voltage aging and temperature-humidity-bias conditions. Embedded capacitors with areas of 0.026 in² (group A) and 0.19 in² (group B) were investigated.

The failure mode during temperature and voltage aging (125°C and 285 V) was found to be a sharp drop in the insulation resistance indicating avalanche breakdown (ABD) and a gradual decrease in capacitance. ABD failures were found to follow two distributions, indicating early life and wearout failures. The MTTFs for early life and wearout life (for the smaller capacitors from group A) were found to be 119 and 452 hrs, respectively. All group B capacitors failed by ABD within 10 hrs. The lower time-to-failure (by ABD) for the larger capacitors can be attributed to an increase in the number of defects in the dielectric with an increase in the area of the capacitor. The nature of degradation of capacitance during aging (125°C and 285 V) was different for small and large capacitors. The degradation of the smaller capacitors (group A) was found to be linear followed by a logarithmic degradation after a certain time (referred to as t_o). The value of the aging transition time t_o was found to be 170.9 ± 5.5 hrs. The larger capacitors (group B) had only a logarithmic degradation region. The effect of area on the degradation in capacitance is currently under investigation. The rate of logarithmic degradation for small and large capacitors was similar implying a change in a material property (possibly dielectric constant) as the reason for logarithmic degradation. The time to 50% failure (as a result of a decrease in capacitance) for group A capacitors was found to be 392 hrs. No failures as a result of a decrease in a capacitance were observed in group B capacitors, during 500 hrs of aging, since the time-to-failure in the logarithmic degradation region is proportional to the initial value of capacitance (the initial value of capacitance of group B capacitors was about one order of magnitude higher than that of group A capacitors).

Under elevated temperature and humidity conditions (85°C and 85% RH for 395 hrs) the capacitance was found to increase by about 15% for both groups of capacitors. Dissipation factor was also found to increase due to moisture absorption in the dielectric. The insulation resistance of this dielectric was stable after application of 5 V at 85°C and 85% RH for 395 hrs. Failures due to a sharp drop in insulation resistance were observed when the applied bias was 150 V under the same environmental conditions.

Temperature and voltage aging and THB tests will continue and further results will be reported in a future publication. Based on the results, recommendations will be provided regarding the design and stress levels for usage of these devices.

8 Acknowledgements

This research was supported by the members of the CALCE Electronic Products and Systems Consortium at the University of Maryland, College Park. The authors would also like to acknowledge Mark Zimmerman at CALCE for his valuable comments on the paper.

9 References:

- [1] A. Madou and L. Martens, "Electrical Behavior of Decoupling Capacitors Embedded in Multilayered PCBs," IEEE Transactions on Electromagnetic Compatibility, pp. 549-556, Vol. 43, No. 4, 2001.
- [2] M. Alam, M. H. Azarian, M. Osterman, and M. Pecht, "Effectiveness of Embedded Capacitors in Reducing the Number of Surface Mount Capacitors for Decoupling Applications," Circuit World, Vol. 36, Issue 1, 2010 (In Press).
- [3] S. Swartz, "Topics in Electronic Ceramics," IEEE Transactions on Electrical Insulation, pp. 935-987, Vol. 25, No. 5, 1990.
- [4] S. Wada, T. Hoshina, H. Yasuno, S. Nam, H. Kakemoto, T. Tsurumi, and M. Yashima, "Size Dependence of Dielectric Properties for nm-Sized Barium Titanate Crystallites and its Origin," Journal of Korean Physical Society, pp. 303-307, Vol. 46, No. 1, 2005.

- [5] K. Jang and K. Paik, "Screen Printable Epoxy/BaTiO₃ Embedded Capacitor Pastes with High Dielectric Constant for Organic Substrate Applications," *Journal of Applied Polymer Science*, pp. 798-807, Vol. 110, 2008.
- [6] K. Paik, J. Hyun, S. Lee, and K. Jang, "Epoxy/BaTiO₃ (SrTiO₃) Composite Films and Pastes for High Dielectric Constant and Low Tolerance Embedded Capacitors in Organic Substrates," 1st Electronics Systemintegration Technology Conference, pp. 794-801, Vol. 2, 2006. Dresden, Germany.
- [7] J. Xu, K. Moon, P. Pramanik, S. Bhattacharya, and C. Wong, "Optimization of Epoxy-Barium Titanate Nanocomposites for High Performance Embedded Capacitor Components," *IEEE Transactions on Components and Packaging Technologies*, pp. 248-253, Vol. 30, No. 2, 2007.
- [8] M. Pecht, L. Nguyen, and E. Hakim, *Plastic Encapsulated Microelectronics*, John Wiley & Sons, New York, NY, 1994.
- [9] W. Mason, "Aging of the Properties of Barium Titanate and Related Ferroelectric Ceramics," *The Journal of the Acoustical Society of America*, pp. 73-85, Vol. 27, No. 1, 1955.
- [10] D. Donahoe, M. Pecht, I. Lloyd, and S. Ganesan, "Moisture Induced Degradation of Multilayer Ceramic Capacitors," *Microelectronics Reliability*, pp. 400-408, Vol. 46, 2006.
- [11] L. Mitoseriu, V. Tura, M. Curteanu, D. Popovici, and A. Anghel, "Aging Effects in Pure and Doped Barium Titanate Ceramics," *IEEE Transactions on Dielectrics and Electrical Insulation*, pp. 500-506, Vol. 8, No. 3, 2001.
- [12] K. Jang and K. Paik, "A Study on Epoxy/BaTiO₃ Embedded Capacitor Pastes for Organic Substrates," *Electronic Components and Technology Conference*, pp. 1504-1509, 2006, San Diego, CA.
- [13] B. Rawal and N. Chan, "Conduction and Failure Mechanisms in Barium Titanate Based Ceramics under Highly Accelerated Conditions," *AVX Technical Report*, Myrtle Beach, SC.
- [14] H. Lee and L. Burton, "Charge Carriers and Time Dependent Currents in BaTiO₃-Based Ceramic," *IEEE Transactions on Components, Hybrids, and Manufacturing Technology*, pp. 469-474, Vol. CHMT-9, No.4, 1986.
- [15] J. Yamamatsu, N. Kawano, T. Arashi, A. Sato, Y. Nakano, and T. Nomura, "Reliability of Multilayer Ceramic Capacitors with Nickel Electrodes," *Journal of Power Sources*, pp. 199-203, Vol. 60, 1996.
- [16] T. Prokopowicz and A. Vaskas, "Research and Development, Intrinsic Reliability, Subminiature Ceramic Capacitors," *Final Report*, ECOM-90705-F, pp. 175, NTIS AD-864068, 1969.
- [17] W. Minford, "Accelerated Life Testing and Reliability of High K Multilayer Ceramic Capacitors," *IEEE Transactions on Components, Hybrids, and Manufacturing Technology*, pp. 297-300, Vol. Chmt-5, No. 3, 1982.
- [18] I. Yoo, L. Burton, and F. Stephenson, "Electrical Conduction Mechanisms of Barium-Titanate-Based Thick-Film Capacitors," *IEEE Transactions on Components, Hybrids, and Manufacturing Technology*, pp. 274-282, Vol. CHMT-10, No. 2, 1987.
- [19] J. Paulsen and E. Reed, "Highly Accelerated Life Testing of Base-Metal-Electrode Ceramic Chip Capacitors," *Microelectronics Reliability*, pp. 815-520, Vol. 42, 2002.
- [20] G. Maher, T. Prokopowicz, and V. Bheemini, "High Volumetric Low Fired X7R MLC Capacitor," 43rd *Proceedings of Electronics Components and Technology Conference*, pp. 280-284, Orlando, FL, 1993.
- [21] M. Randall, A. Gaurav, D. Skamsner, and J. Beeson, "Lifetime Modeling of Sub 2 Micron Dielectric Thickness BME MLCC," *Proceedings of Capacitor and Resistor Technology Symposium*, pp. 1-7, Scottsdale, AZ, 2003.
- [22] R. Das, J. Lauffer, and V. Markovich, "Fabrication, Integration and Reliability of Nanocomposite Bases Embedded Capacitors in Microelectronics Packaging," *Journal of Materials Chemistry*, pp. 537-544, Vol. 18, 2008.
- [23] S. Lee, J. Hyun, J. Pak, H. Lee, H. Jeon, and K. Paik, "Fabrication and Characterization of Embedded Capacitors in Printed Circuit Boards Using B-Stage Epoxy/BaTiO₃ Composite Embedded Capacitor Films (ECFs)," *Electronic Components and Technology Conference*, pp. 742-746, Lake Buena Vista, Florida, USA, 2008.

- [24] C. Zou, J. Fothergill, and S. Rowe, "The Effect of Water Absorption on the Dielectric Properties of Epoxy Nanocomposites," *IEEE Transactions on Dielectrics and Electrical Insulation*, pp. 106-117, Vol. 15, No. 1, 2008.
- [25] M. Alam, M. H. Azarian, M. Osterman, and M. Pecht, "Reliability of Embedded Planar Capacitors under Temperature and Voltage Stress," *Proceedings of Capacitor and Resistor Technology Symposium*, Jacksonville, FL, USA, 2009.



Comparative Analysis of Solder Joint Degradation using RF Impedance and Event Detectors

Daeil Kwon, Michael H. Azarian, and Michael Pecht

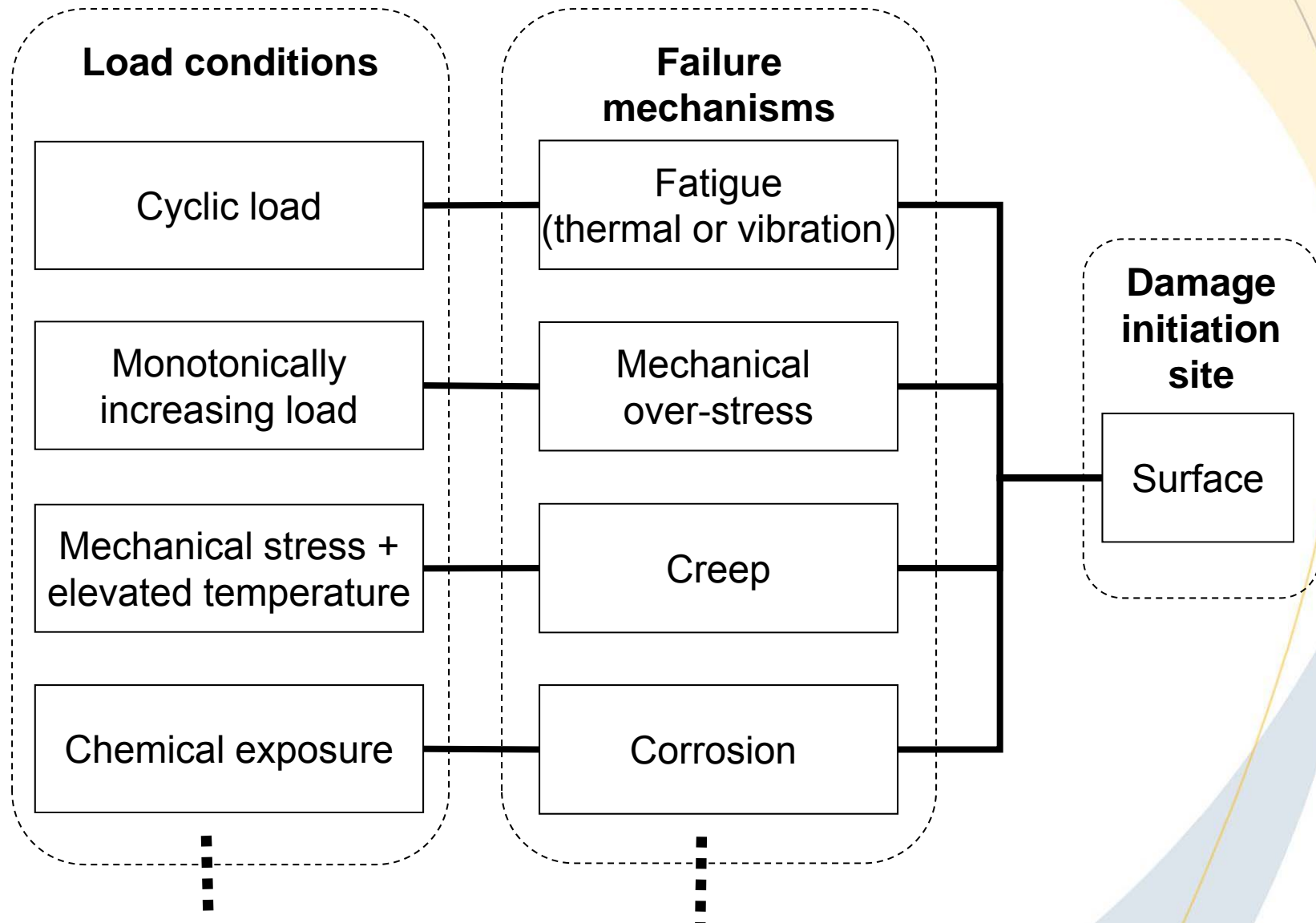
Center for Advanced Life Cycle Engineering (CALCE)

University of Maryland
College Park, MD 20742
www.calce.umd.edu

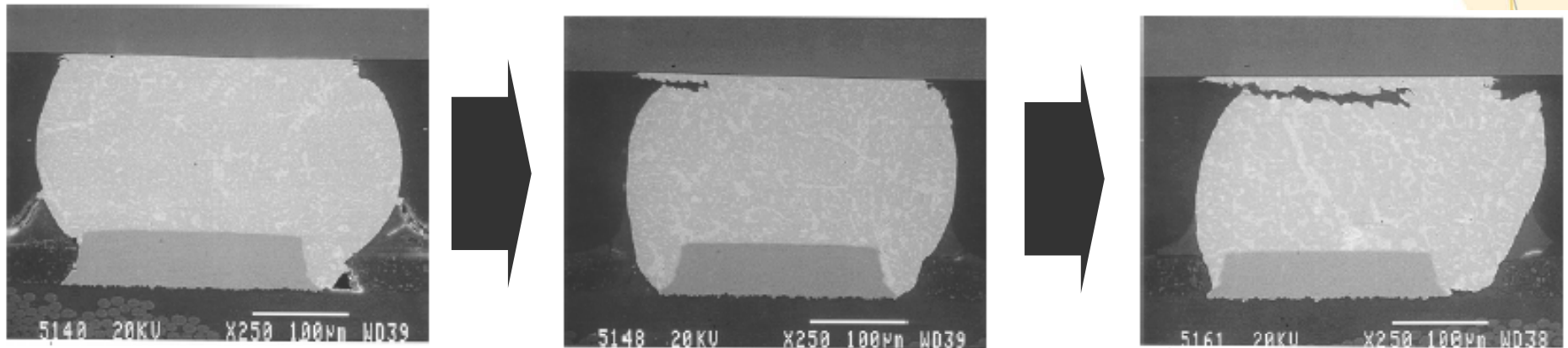
Email: mazarian@calce.umd.edu

Tel: (301) 405-5323

Typical Causes of Solder Joint Failure



The Role of the Interconnect Surface in Early Stages of Degradation

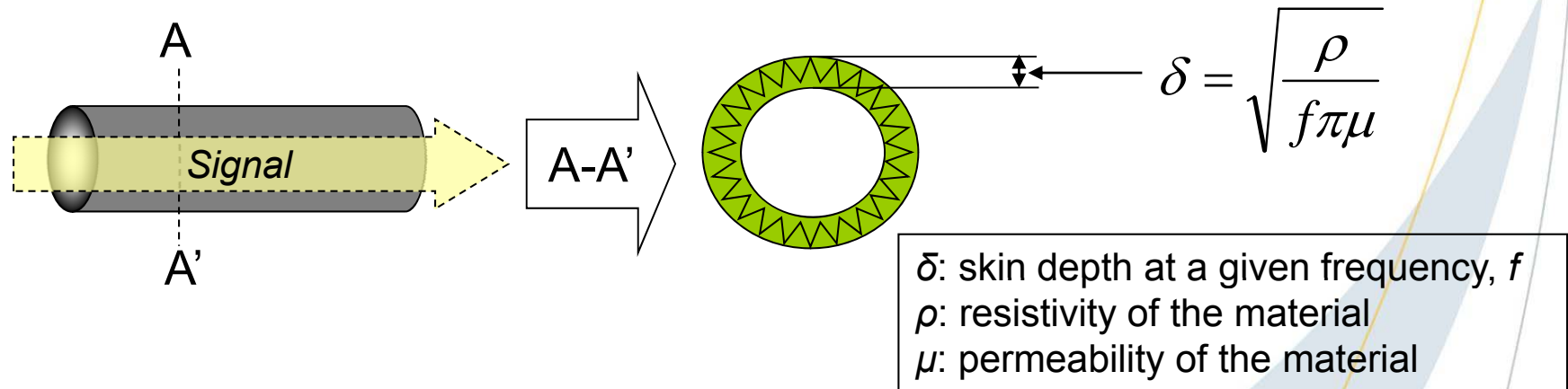


Interconnect degradation often starts from the surface and propagates inward.

Ref.: Kim and Elenius, Proc. of 51st ECTC, 2001, pp. 681-686.

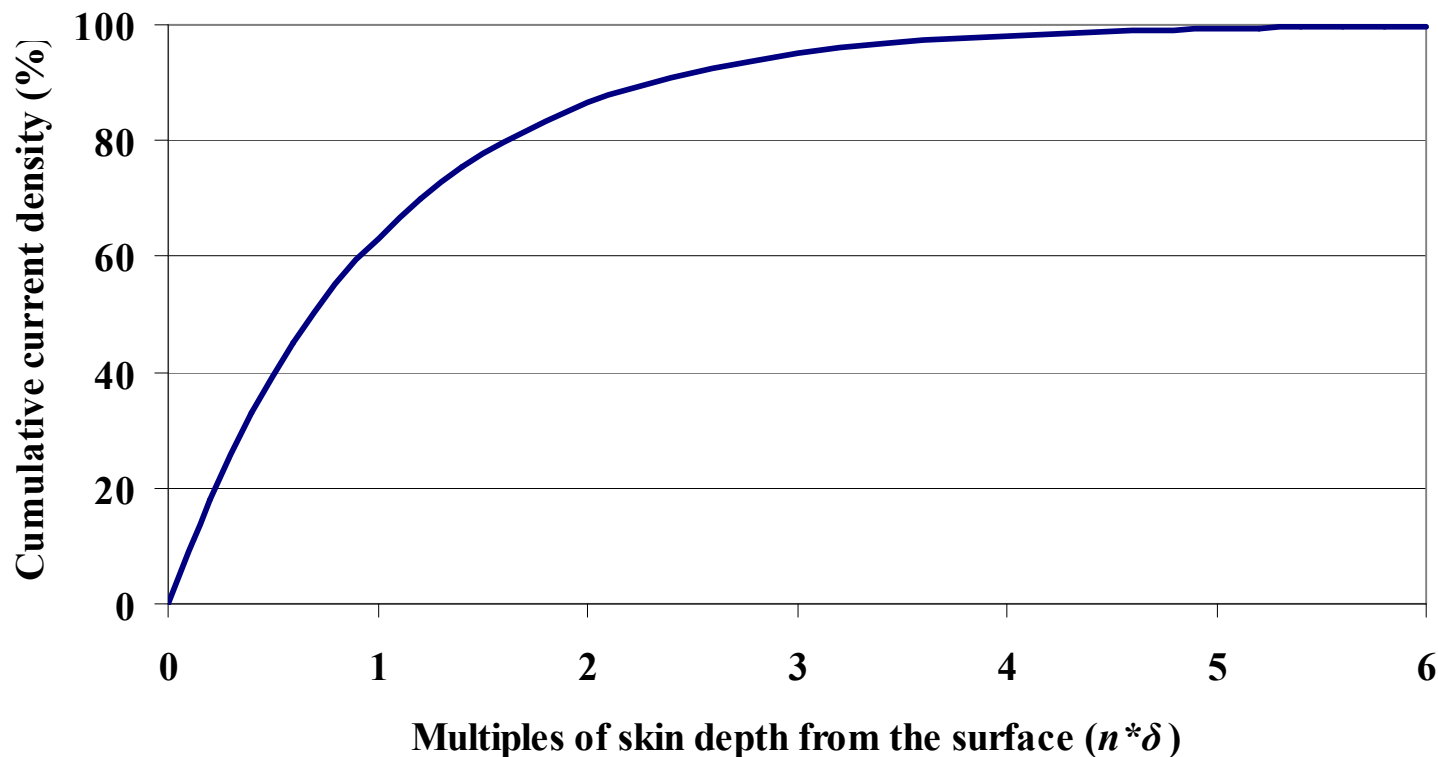
Sensitivity of Signal Propagation to Interconnect Degradation

- At high operating frequencies, signal propagation is concentrated at the surface of interconnects. This phenomenon is referred to as the “skin effect.”
- Due to the skin effect, even a small crack initiated at the surface of an interconnect raises the RF impedance.
- Therefore, RF impedance provides an improved means of monitoring interconnect degradation.



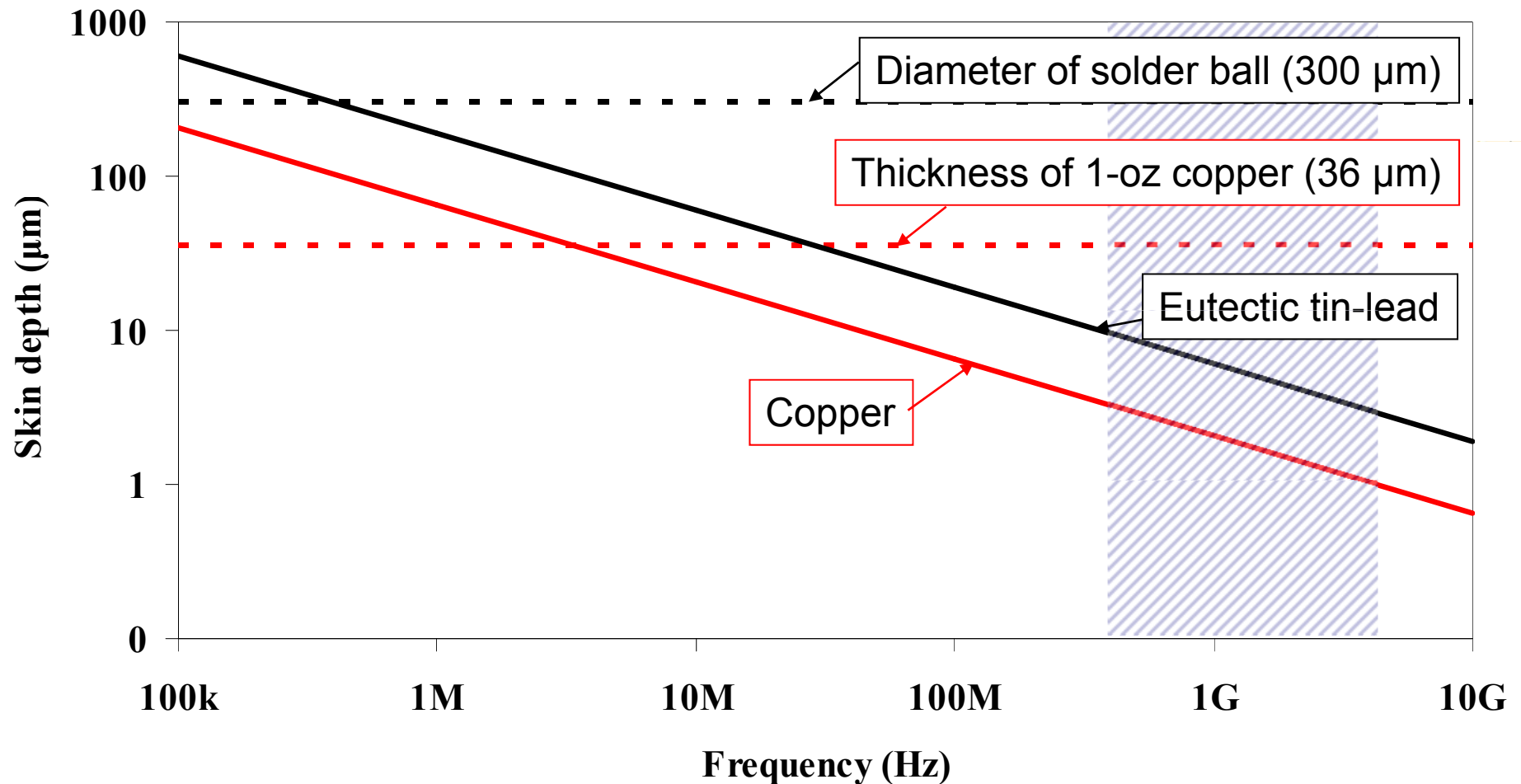
Cumulative Current Density with Depth

- The skin depth, δ , is the distance from the surface within which about 63% of the current is concentrated.
- Due to the skin effect, more than 99% of the current is concentrated within five skin depths from the surface.



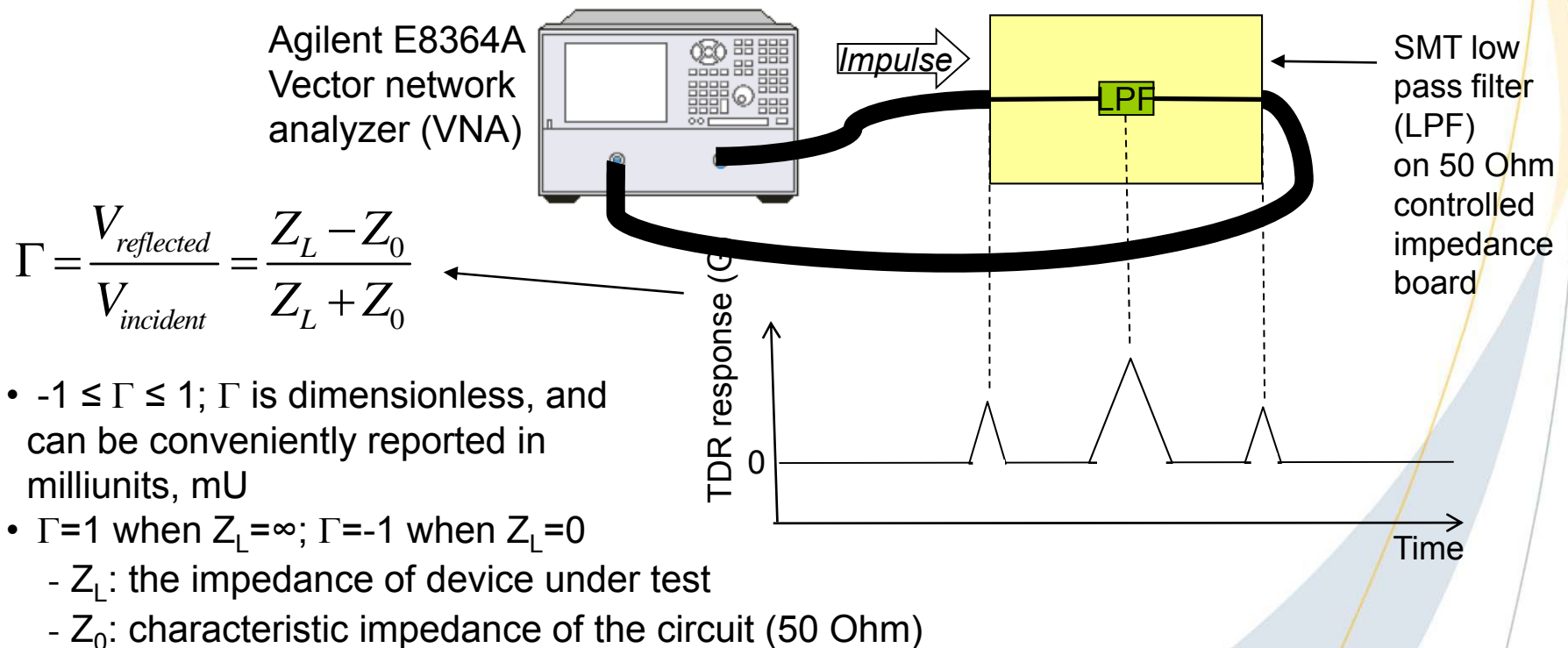
Skin Depth of Interconnects

At frequencies over about 500 MHz, skin depth becomes less than a tenth of interconnect size.



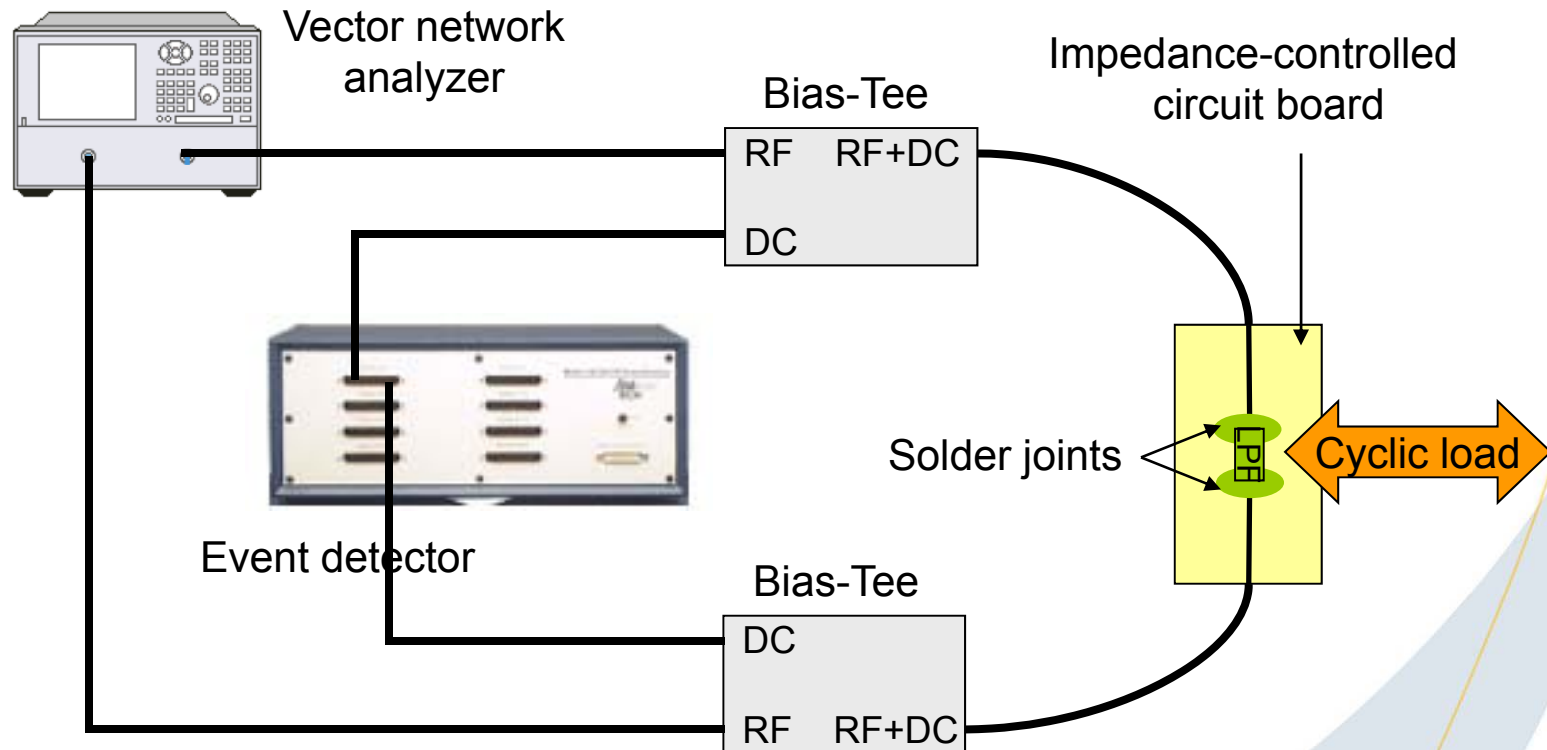
Time Domain Reflectometry (TDR)

- TDR reflection coefficient (Γ) is the ratio of the incident and reflected voltage due to impedance discontinuities in the circuit.
- In the time domain, any discontinuities due to impedance mismatches within the circuit are seen as discrete peaks.
- TDR reflection coefficient is used as a measure of RF impedance.

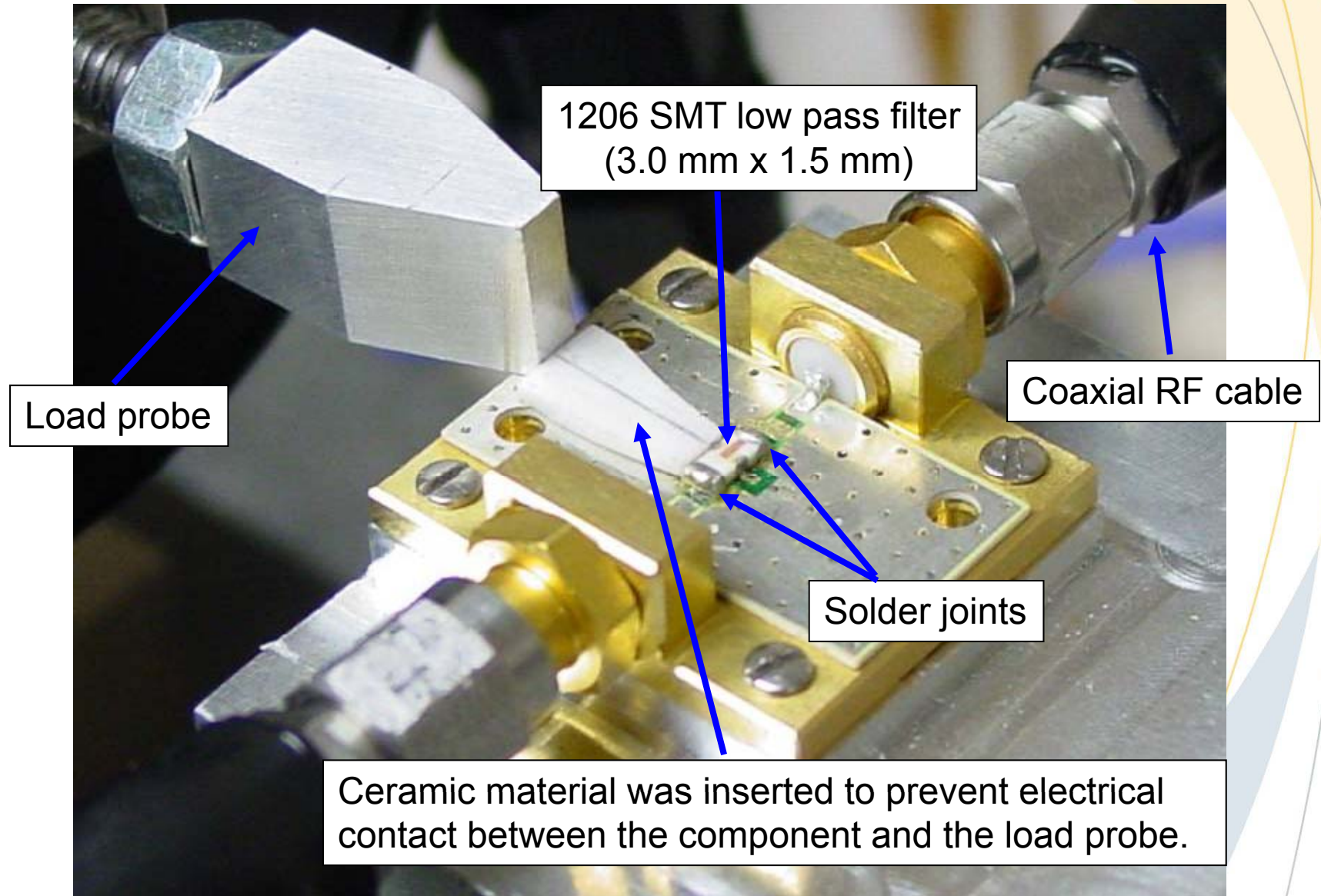


Schematic for Fatigue Tests

- Controlled cyclic load was applied to generate fatigue failure of the solder joints.
- During fatigue tests, RF impedance and DC resistance were simultaneously monitored using a VNA and an event detector, respectively.

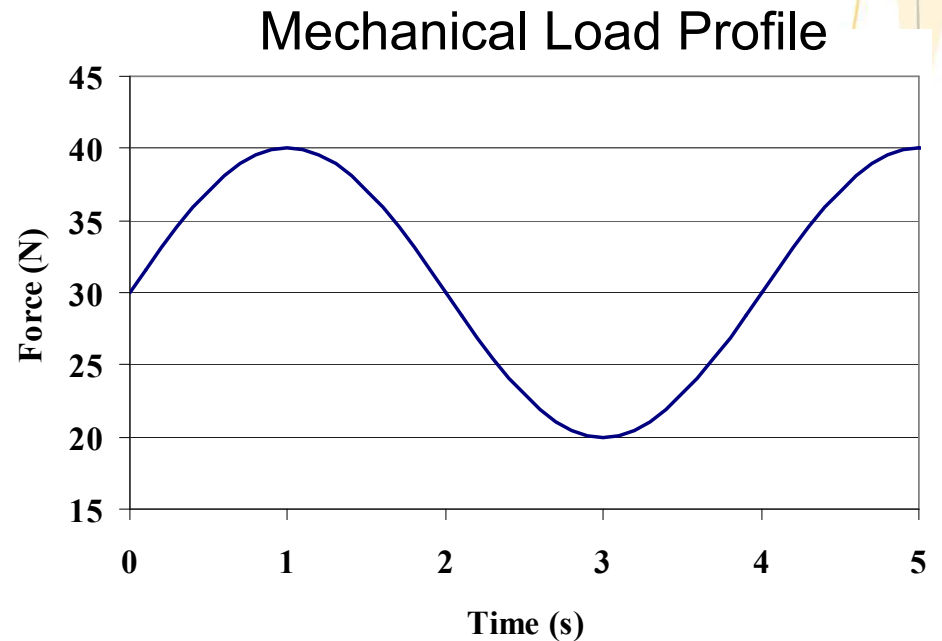


Experimental Setup



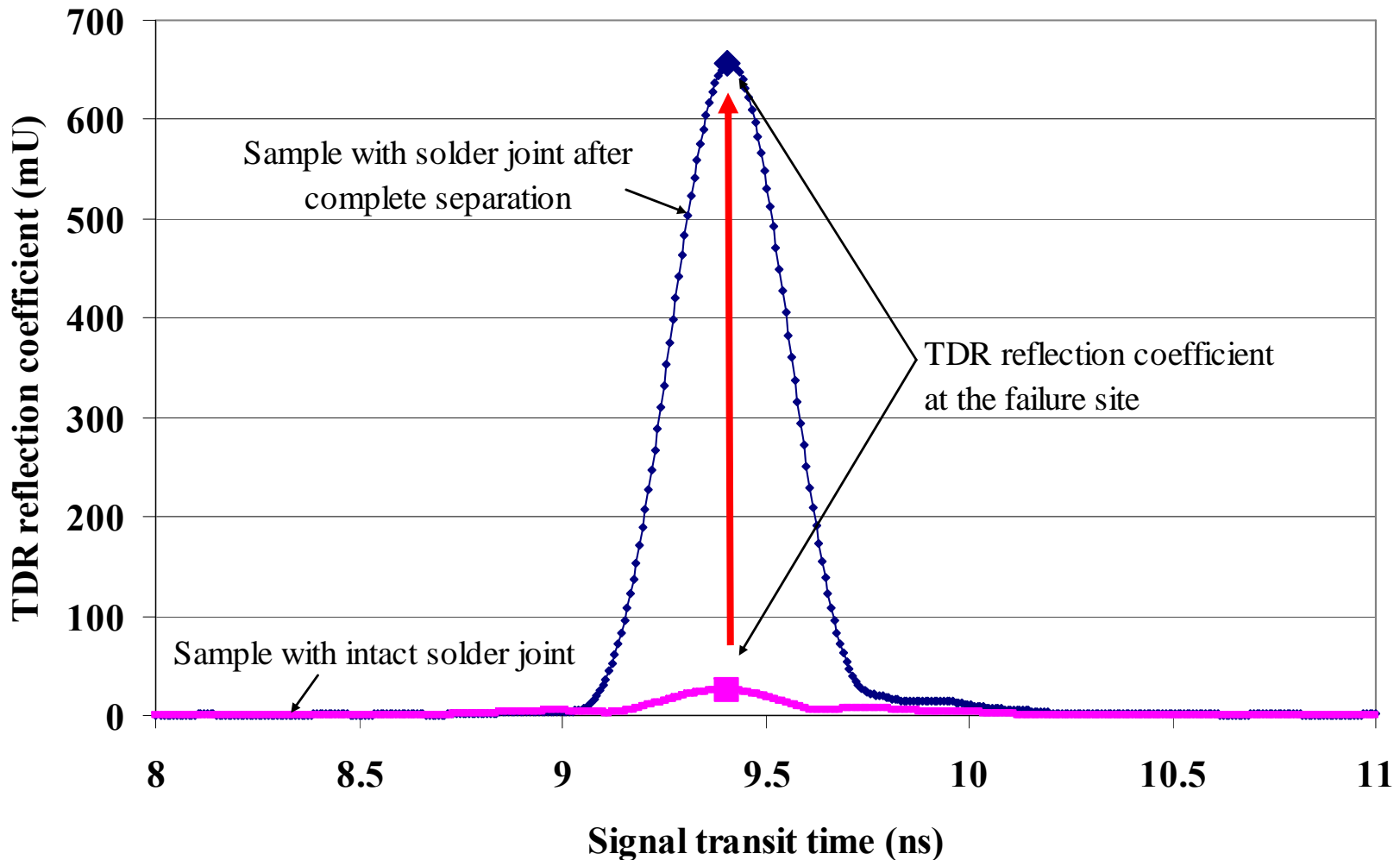
Fatigue Test Conditions

- Equipment
 - MTS Tytron 250 (load unit)
 - Agilent E8364A vector network analyzer (RF measurement)
 - AnalysisTech Event Detector STD128 (DC measurement)
- Electrical characteristics
 - Cut-off frequency of the low pass filter: 6.7 GHz
 - Characteristic impedance: 50 Ohms
- Test variables
 - RF frequency range:
500 MHz ~ 6 GHz
 - Mean and amplitude force for cyclic loading: 30 N and 10 N
 - Load frequency: 0.25 Hz
 - Data acquisition interval:
every 30 sec



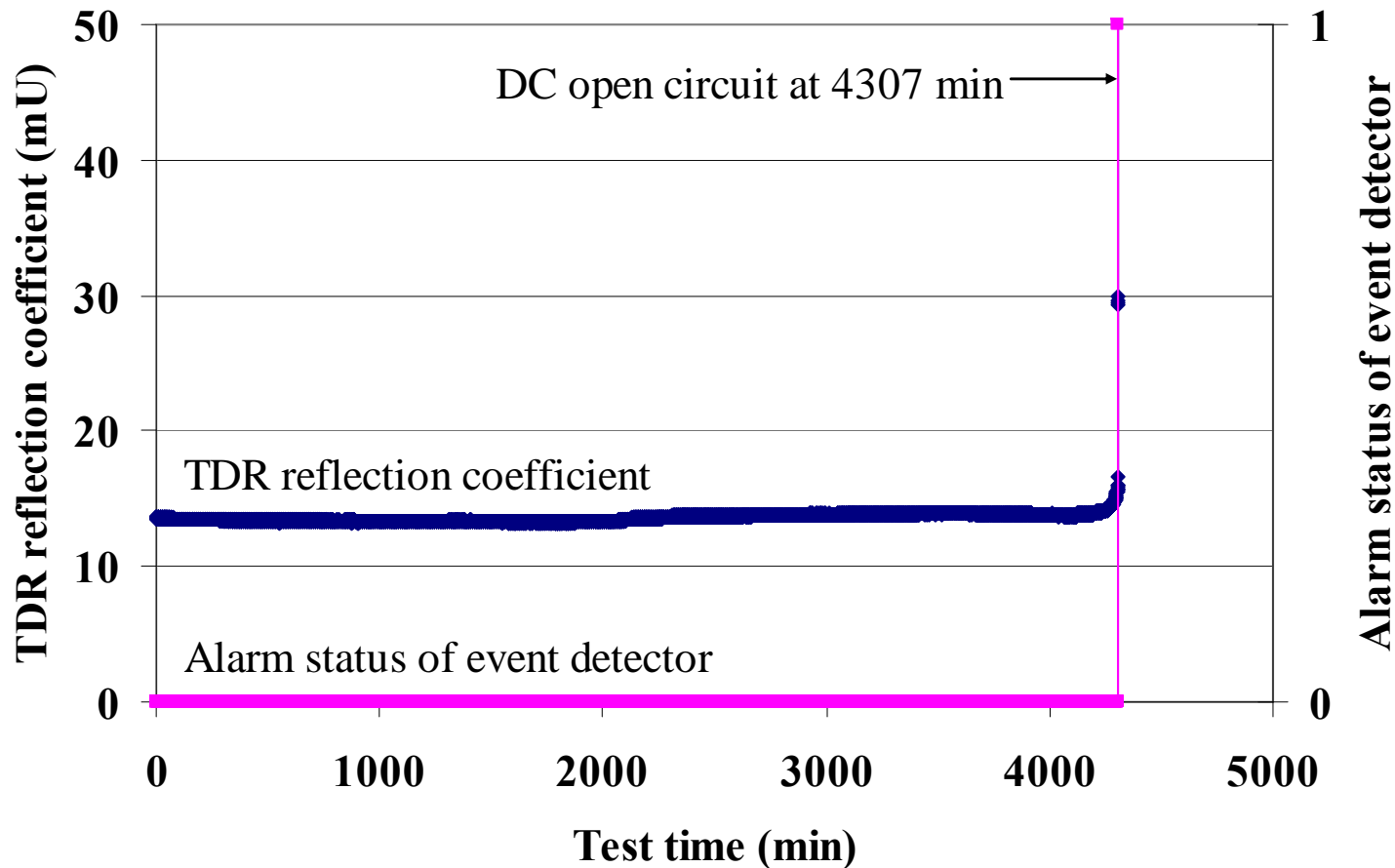
TDR Reflection Coefficient Measurements

TDR reflection coefficients at the solder joint were extracted from the collected TDR data to examine their changes.



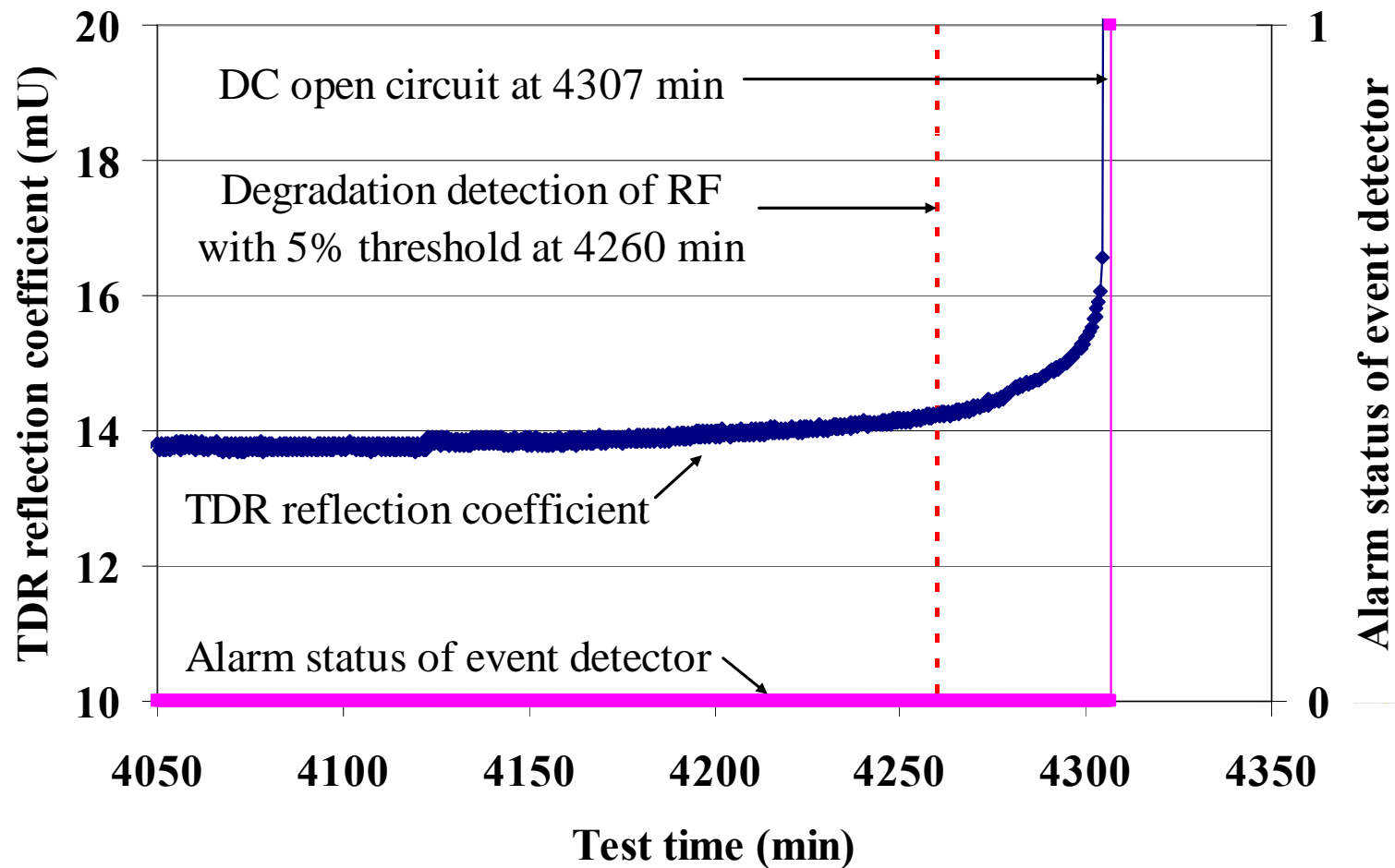
RF Precursor Earlier than Event Detector

- Toward the end of the tests, the TDR reflection coefficient provided failure precursors as a gradual increase.
- On the other hand, the event detector did not trigger any alarms until a DC open circuit occurred.



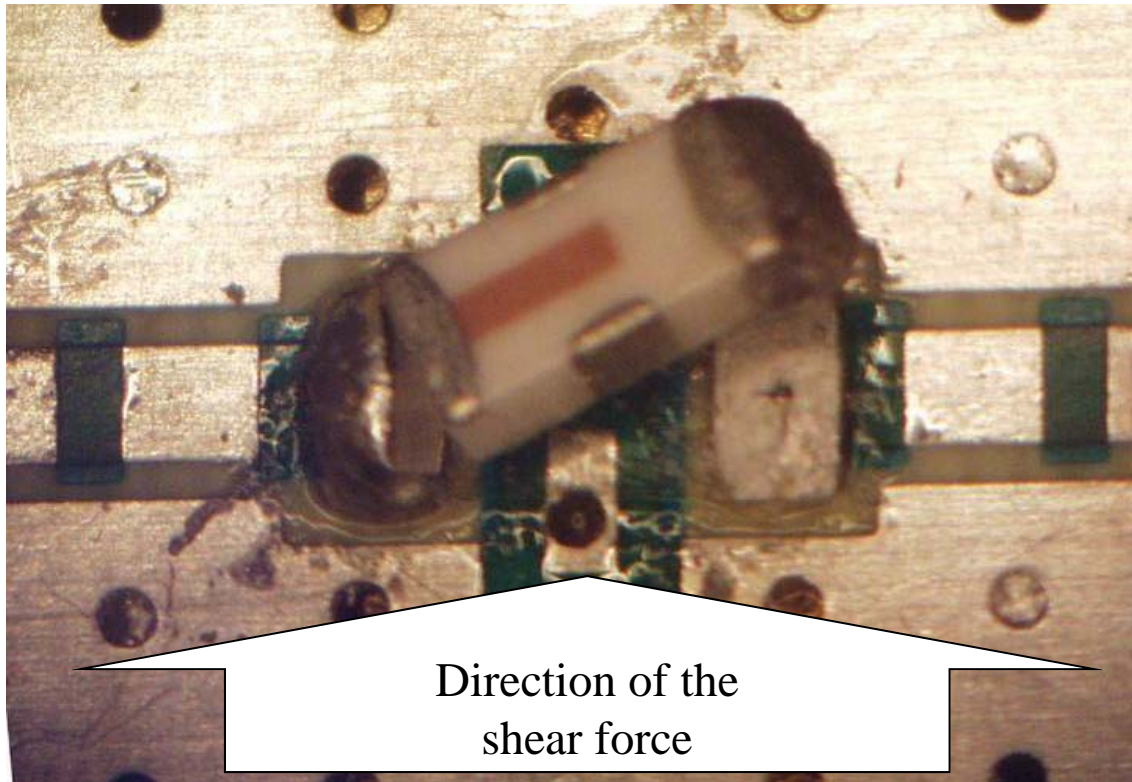
Comparison of Detection Sensitivity

A 5% increase of the initial value occurred at 4260 minutes, which was 47 minutes earlier than the time to failure based on the event detector.



Cracked Solder Joint

The direction of the solder joint separation coincided with that of the applied shear force.





Consistency of Early Detection Using RF Impedance

In general, the same behaviors of the TDR reflection coefficient and the event detector measurement were consistently observed over multiple trials, along with the confirmation of the same failure mechanism, solder joint cracking.

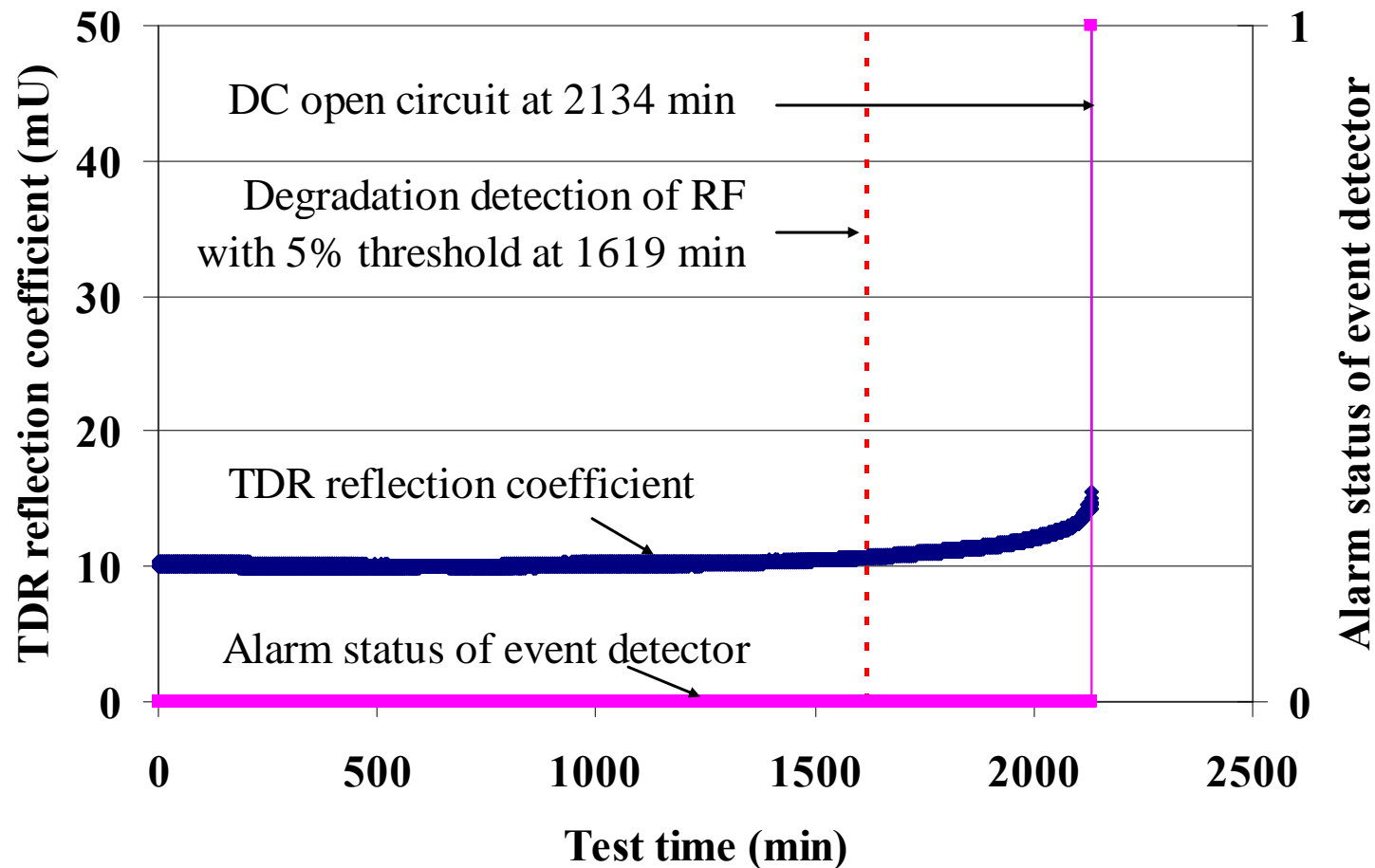
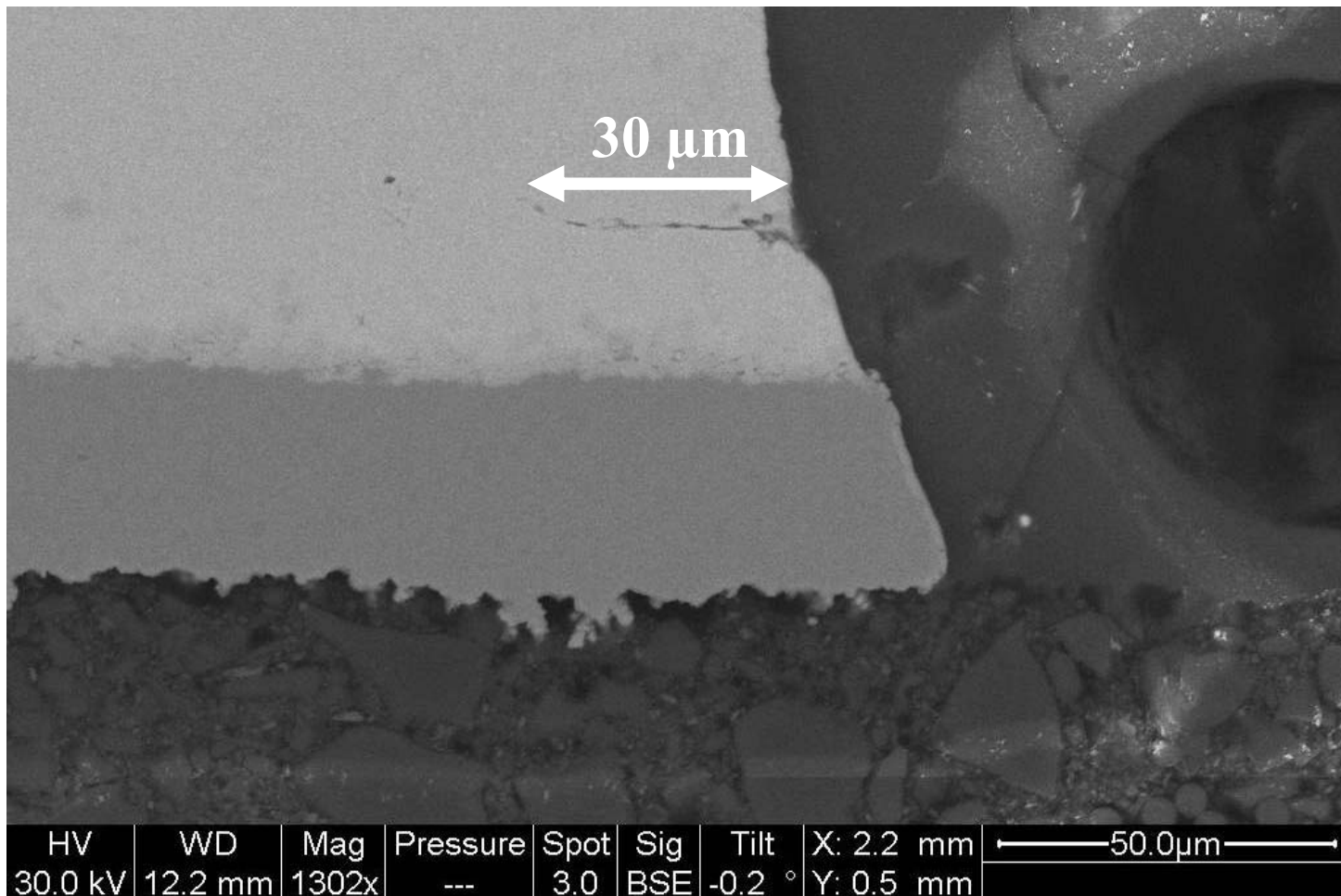




Illustration of Sensitivity of RF Impedance to Interconnect Degradation

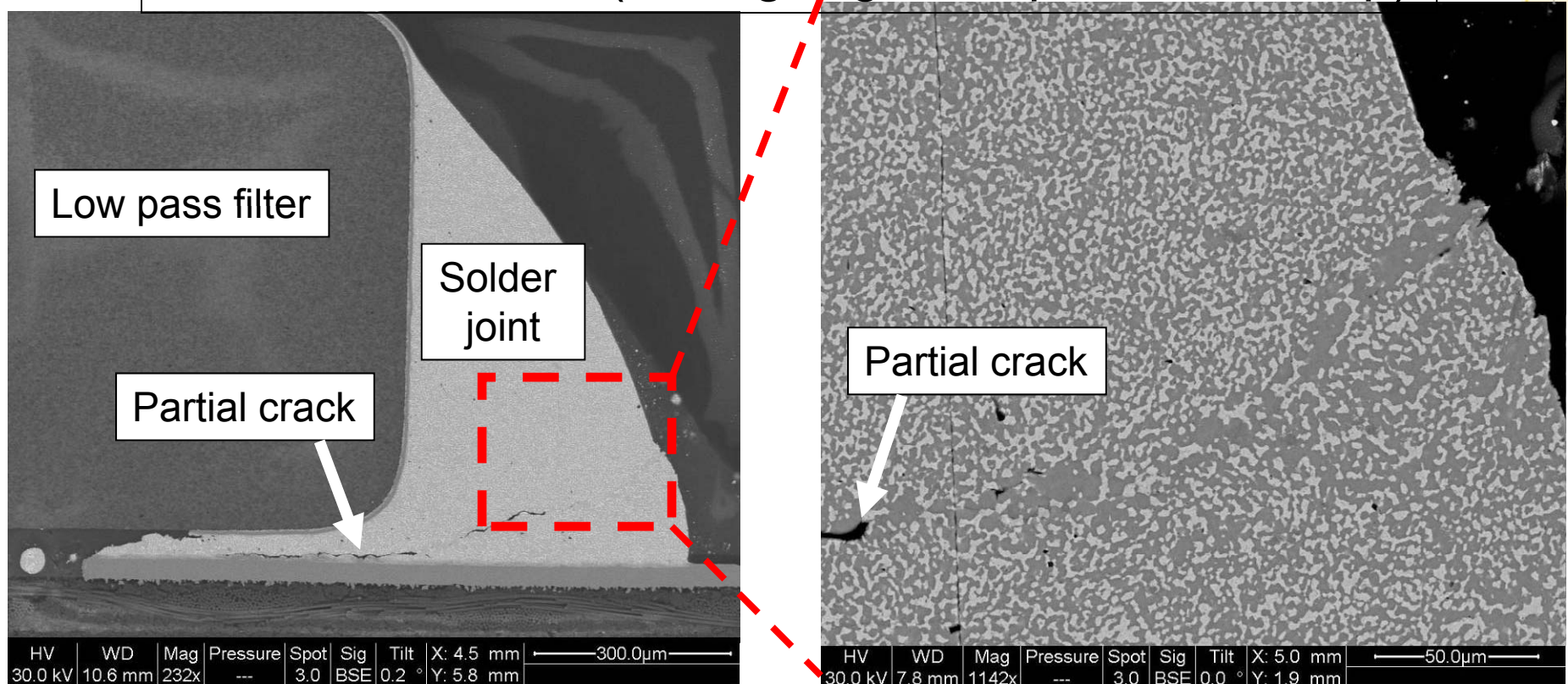
Using a statistical anomaly detection technique to improve sensitivity, RF impedance can detect a partial crack of only 30 μm within a solder joint.



Application of RF Impedance Monitoring to Studies of Damage Accumulation

- The RF response is well-behaved and directly correlated to crack growth, providing a real-time, non-destructive monitoring tool.
- In this example, the geometry and the localized changes to the microstructure strongly suggest the future crack path.

SnPb Solder Joint (During High Temperature Creep)



Conclusions

- RF impedance can provide a more sensitive means to diagnose solder joint degradation than do measurements based on DC resistance, such as event detectors.
 - RF impedance changes are consistently detectable prior to event detector alarms under cyclic loading conditions.
 - RF impedance does not require high speed data acquisition in order to detect failure precursors.
- RF impedance appears to be the most sensitive and consistent hardware solution available for early warning of interconnect failure.
 - RF impedance can accurately assess the reliability of high speed electronic products, which are sensitive to even minor levels of interconnect damage.



Benefits of the Technique Include ...

- Real-time monitoring of interconnect degradation, providing non-destructive early warning of impending failure.
- A tool for the study of damage accumulation processes during interconnect degradation.
- A basis for prognostics of electronic products, enabling
 - reliable prediction of the remaining useful life of interconnects;
 - condition-based maintenance; and
 - improved safety and reduced life-cycle costs.



Thank you for your attention.

